

A universally enhanced light-quarks Yukawa couplings paradigm

Shaouly Bar-Shalom^{1,*} and Amarjit Soni^{2,†}

¹*Physics Department, Technion-Institute of Technology, Haifa 32000, Israel*

²*Physics Department, Brookhaven National Laboratory, Upton, NY 11973, USA*

(Dated: November 8, 2021)

We propose that natural TeV-scale new physics (NP) with $\mathcal{O}(1)$ couplings to the standard model (SM) quarks may lead to a universal enhancement of the Yukawa couplings of all the light quarks, perhaps to a size comparable to that of the SM b-quark Yukawa coupling, i.e., $y_q \sim \mathcal{O}(y_b^{SM})$ for $q = u, d, c, s$. This scenario is described within an effective field theory (EFT) extension of the SM, for which a potential contribution of certain dimension six effective operators to the light quarks Yukawa couplings is $y_q \sim \mathcal{O}\left(f \frac{v^2}{\Lambda^2}\right)$, where v is the Higgs vacuum expectation value (VEV), $v = 246$ GeV, Λ is the typical scale of the underlying heavy NP and f is the corresponding Wilson coefficient which depends on its properties and details. In particular, we study the case of $y_q \sim 0.025 \sim y_b^{SM}$, which is the typical size of the enhanced light-quark Yukawa couplings if the NP scale is around $\Lambda \sim 1.5$ TeV and the NP couplings are natural, i.e., $f \sim \mathcal{O}(1)$. We also explore this enhanced light quarks Yukawa paradigm in extensions of the SM which contain TeV-scale vector-like quarks and we match them to the specific higher dimensional effective operators in the EFT description. We discuss the constraints on this scenario and the flavor structure of the underlying NP dynamics and suggest some resulting “smoking gun” signals that should be searched for at the LHC, such as multi-Higgs production $pp \rightarrow hh, hhh$ and single Higgs production in association with a high p_T jet (j) or photon $pp \rightarrow h j, h\gamma$ and with a single top-quark $pp \rightarrow ht$.

I. INTRODUCTION

After the discovery of the 125 GeV Higgs-like boson, one of the main tasks of the current and future runs of the LHC is to uncover its properties and the physics which underlies its origin. This has led to considerable effort from both the theoretical and experimental sides, in the hunt for the NP which may address fundamental questions in particle physics, possibly related to the scalar sector of the SM, such as the observed hierarchy between the two disparate Planck and EW scales and the flavor and CP structure in the fermion sector.

The Higgs mechanism of the SM suggests that the Yukawa couplings of the fermions are proportional to the ratio between their masses and the Higgs VEV ($v = 246$ GeV), i.e., $y_f \propto m_f/v$. In particular, for the light fermions where m_f/v is vanishingly small, reactions involving their interaction with the Higgs boson are in many cases expected to be strongly suppressed and unobservable in the SM. Therefore, any observable signal which can be associated with an enhanced Yukawa coupling of a light fermion would stand out as clear evidence for NP beyond the SM. Indeed, current experimental bounds and Higgs measurements do not exclude the possibility that the Yukawa sector of the SM is modified by TeV-scale NP that directly affects the couplings of the observed 125 GeV Higgs; the current bounds do not exclude Yukawa couplings of the Higgs to the light quarks of the order of the b-quark Yukawa coupling, i.e., allowing $y_q \sim \mathcal{O}(y_b^{SM})$ for $q = d, u, s, c$ [1–6].

In this work we propose a framework where the Yukawa interactions of all the light quarks are universally enhanced, naming it the “Universally Enhanced Higgs Yukawa” paradigm - UEHiggsY paradigm. In particular, we suggest that, if the pattern and size of the Higgs Yukawa interaction Lagrangian is controlled by some TeV-scale underlying NP with natural couplings of $\mathcal{O}(1)$, then $y_q \sim \mathcal{O}(y_b^{SM})$ can be universally realized for all $q = d, u, s, c, b$. We first describe the UEHiggsY paradigm based on an EFT approach and then give an explicit implementation of this mechanism within a renormalizable prescription involving new TeV-scale vector-like quarks (VLQ) with natural $\mathcal{O}(1)$ Yukawa-like couplings to the SM quarks.

II. AN EFT DESCRIPTION OF THE UEHIGGSY PARADIGM

Consider the effective Lagrangian piece corresponding to one of the simplest dimension six effective operators that can generate non-SM Yukawa-like terms:

$$\Delta \mathcal{L}_{qH} = \frac{H^\dagger H}{\Lambda^2} \cdot \left(f_{uH} \bar{q}_L \tilde{H} u_R + f_{dH} \bar{q}_L H d_R \right) + h.c. , \quad (1)$$

where H ($\tilde{H} \equiv i\tau_2 H^*$), q_L and u_R, d_R are the SU(2) SM Higgs, left-handed quark doublets and right-handed quark singlets, respectively. Also, Λ is the NP scale and f_i are the corresponding Wilson coefficients which depend on the details of the underlying NP theory.

When the above dimension six operators are added to the SM Yukawa interaction Lagrangian:

$$\mathcal{L}_{SM}^Y = -Y_u \bar{q}_L \tilde{H} u_R - Y_d \bar{q}_L H d_R + h.c. , \quad (2)$$

*Electronic address: shaouly@physics.technion.ac.il

†Electronic address: adlersoni@gmail.com

and EW symmetry is spontaneously broken, one obtains the quark mass matrices \tilde{M}_q ($q = u, d$ for up and down quarks, respectively) and the Yukawa couplings in the weak basis. The physical quark masses, M_q , are then obtained by unitary rotations of both the left and right-handed quark fields to the quarks mass basis, $q_{L,R} \rightarrow S_{L,R}^q q_{L,R}$ (the CKM matrix is $V = S_L^{u\dagger} S_L^d$): $M_d \equiv S_L^{d\dagger} \tilde{M}_d S_R^d = \text{diag}(m_d, m_s, m_b)$ and $M_u \equiv S_L^{u\dagger} \tilde{M}_u S_R^u = \text{diag}(m_u, m_c, m_t)$, where:

$$M_q = \frac{v}{\sqrt{2}} \left(\hat{Y}_q - \frac{1}{2} \epsilon \hat{f}_{qH} \right) ; \epsilon \equiv \frac{v^2}{\Lambda^2} , \quad (3)$$

and couplings in the physical quark mass basis are denoted with a hat: $\hat{Y}_q \equiv (S_L^q)^\dagger Y_q S_R^q$ and $\hat{f}_{qH} \equiv (S_L^q)^\dagger f_{qH} S_R^q$.

The Yukawa couplings, $y_q^{ij} \bar{q}_i q_j h$, are then given by:

$$y_q^{ij} = \frac{m_q}{v} \delta_{ij} - \frac{\epsilon}{\sqrt{2}} \left(\hat{f}_{qH}^{ij} R + \hat{f}_{qH}^{ji\star} L \right) , \quad (4)$$

where m_q is the physical quark mass and $R(L) = (1 + (-)\gamma_5)/2$.

It is, therefore, evident from Eq. 4 that our UEHiggsY paradigm is realized if the NP operators in Eq. 1 are natural, i.e., if $f_{qH} \sim \mathcal{O}(1)$, and have a typical scale of $\Lambda \sim \mathcal{O}(1 \text{ TeV})$. More specifically, taking $\Lambda \sim 1.3 \text{ TeV}$ and $\hat{f}_{qH} \propto f_{qH} \sim \mathcal{O}(1)$, we have $\epsilon \hat{f}_{qH} \sim 0.035$, thus leading to the UEHiggsY scenario:

$$y_q \sim \frac{\epsilon}{\sqrt{2}} \hat{f}_{qH} \sim 0.025 \sim y_b^{SM} , \quad (5)$$

for all the light quarks ($q = d, u, s, c$) where $m_q/v \ll \epsilon \hat{f}_{qH}$, as well as for the b-quark for which $m_b/v \sim \epsilon \hat{f}_{qH}$.^[1]

We note that our UEHiggsY setup which yields the modified Yukawa couplings of Eq. 4, also allows for a very small b-quark Yukawa coupling as well as for negative Yukawa couplings for all light quarks including also the b-quark. Indeed, a suppressed b-quark Yukawa, e.g., of the size of the SM d-quark Yukawa, $y_b \sim y_d^{SM}$, requires some degree of cancellation between the EFT contribution (with $\hat{f} \sim \mathcal{O}(1)$) and the SM Yukawa term (with $\hat{Y}_q \sim \mathcal{O}(y_b^{SM})$) to the level of m_d/m_b (see also [8, 46]). As discussed below, this fine-tuning is not worse than the typical fine-tuning required for the UEHiggsY paradigm, e.g., to obtain $y_d \sim \mathcal{O}(y_b^{SM})$. Also, the sign of the Yukawa couplings in the UEHiggsY setup depends on the sign of the Wilson coefficients, in particular for the light quarks $q = u, d, c, s$ for which $m_q/v \ll \epsilon \cdot \hat{f}_{qH}$ when $\Lambda \sim \mathcal{O}(1) \text{ TeV}$ and $\hat{f}_{qH} \sim \mathcal{O}(1)$. We note, however, that the dependence of the UEHiggsY signals studied in

section V on the sign of the enhanced y_q is mild, since interference effects with the SM are sub-dominant in these processes.

In addition to the modification of the light quarks Yukawa couplings, the effective operators in Eq. 1 also generate new tree-level contact interactions between the SM light quarks and two or three Higgs particles, $q\bar{q}hh$ and $q\bar{q}hhh$. These new couplings are also proportional to \hat{f}_{qH} :

$$\Gamma_{\bar{q}_i q_j hh} = \frac{3\epsilon}{\sqrt{2}v} \left(\hat{f}_{qH}^{ij} R + \hat{f}_{qH}^{ji\star} L \right) , \quad \Gamma_{\bar{q}_i q_j hhh} = \frac{\Gamma_{\bar{q}_i q_j hh}}{v} . \quad (6)$$

and may cause large deviations (from the expected SM rates) to the multi-Higgs production channels $pp \rightarrow hh, hhh$ at the LHC, as will be discussed in section V.

The above UEHiggsY paradigm suffers, however, from two potential problems associated with fine-tuning and flavor:

fine-tuning: Some degree of fine-tuning is required among the parameters of the Lagrangian pieces $\mathcal{L}_{SM}^Y + \Delta \mathcal{L}_{qH}$ in order to simultaneously accommodate the light-quark masses $m_q \ll m_b$ and the enhanced Yukawa couplings of $y_q \sim \mathcal{O}(y_b^{SM})$. As will be discussed below, this fine-tuning is, however, not worse than the flavor fine-tuning in the SM.

flavor: The Yukawa couplings Y_q and Wilson coefficients f_{qH} cannot be diagonalized simultaneously in general. As a result, flavor changing neutral couplings (FCNC) among the SM quarks may appear. This is manifested by the off-diagonal elements of \hat{f}_{qH} (see Eq. 4), which are a-priori expected to be of $\mathcal{O}(1)$. In particular, with $\Lambda \sim \mathcal{O}(1) \text{ TeV}$, we obtain FCNC $q_i q_j h$ couplings also of the size of the b-quark Yukawa, e.g., $y_q^{ij} \sim \epsilon \hat{f}_{qH}^{ij}/\sqrt{2} \sim \mathcal{O}(y_b^{SM})$ for $i = 1, j = 2$ (see Eq. 5). We will address this flavor problem in the next section.

As for the fine-tuning issue, it is typically of the order of m_q/m_b , so that the worst fine-tuning corresponds to the 1st generation quarks, where it is $\sim \mathcal{O}(m_{u,d}/m_b) \sim 10^{-3}$. To see that, consider the mass and Yukawa coupling of a single light quark q in the presence of the interactions terms in $\mathcal{L}_{SM}^Y + \Delta \mathcal{L}_{qH}$:

$$m_q = \frac{v}{\sqrt{2}} \left(Y_q - \frac{1}{2} \epsilon f_{qH} \right) , \quad (7)$$

$$y_q = \frac{1}{\sqrt{2}} \left(Y_q - \frac{3}{2} \epsilon f_{qH} \right) . \quad (8)$$

In particular, fixing m_q to its measured/observed value (e.g., $m_q \sim 2 \text{ MeV}$ for the u-quark) and requiring that $y_q \sim y_b^{SM} = \sqrt{2}m_b/v \sim 0.025$, the solution to Eqs. 7 and

[1] Note that $y_q \sim y_c^{SM}$ would be the natural choice of the UEHiggsY framework if the NP scale is around 2.5 TeV.

8 for the corresponding couplings Y_q and f_{qH} is:

$$Y_q = -\frac{y_b^{SM}}{\sqrt{2}} \left(1 - \frac{3}{\sqrt{2}} \frac{m_q}{m_b} \right), \quad (9)$$

$$\epsilon f_{qH} = -\sqrt{2} y_b^{SM} \left(1 - \frac{1}{\sqrt{2}} \frac{m_q}{m_b} \right). \quad (10)$$

Thus, both ϵf_{qH} and Y_q need to be of $\mathcal{O}(y_b^{SM})$ and the resulting fine-tuning is at the level of $\Delta_q \sim \mathcal{O}(m_q/m_b)$. We therefore see that the UEHiggsY paradigm which arises from natural TeV-scale NP with $\mathcal{O}(1)$ couplings, requires technical fine-tuning of the quark-Higgs interaction parameters at the level of $\Delta_q \sim \mathcal{O}(0.1, 0.01, 0.001)$ for $q = c, s, u/d$, respectively. In particular, the fine-tuning is at most at the per-mill level and is only technical in the sense that the fine-tuned parameters, once fixed, are stable against higher-order corrections (as opposed to the fine-tuning in the SM Higgs potential). In fact, this technical $10^{-3} - 10^{-1}$ fine-tuning is comparable to the flavor fine-tuning problem in the SM, which is manifest in the CKM matrix that has no a-priori reason to be close to the identity matrix [9].

III. THE UNDERLYING HEAVY PHYSICS AND FLAVOR

The effective operators in Eq. 1 can be generated by various types of heavy underlying NP which contain new heavy particles that couple to the SM fermions. In Fig. 1 we depict examples of tree-level diagrams in the underlying theory, which can generate the dimension 6 effective operators of Eq. 1 when the heavy fields are integrated out. In particular, the underlying NP theory may contain heavy VLQ (F_1 and F_2) and/or a heavy scalar (Φ) - both have the required quantum numbers to couple to the SM quarks and Higgs fields. Indeed, new heavy scalars and/or vector-like fermions are elementary building blocks of several well motivated beyond the SM scenarios which may address fundamental unresolved theoretical questions in particle physics.

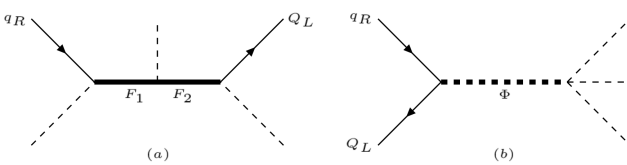


FIG. 1: Tree-level diagrams in the underlying heavy theory which can generate the dimension 6 operators in Eq. 1, involving exchanges of heavy VLQ F_1, F_2 (left) and a heavy scalar Φ (right). See also text.

As an example for a simple occurrence of the UEHiggsY framework, we will focus below on the heavy VLQ

scenario, which has rich phenomenological implications [10–19] and may be linked to the mechanism responsible for solving the hierarchy problem [20], as well as to naturalness issues in supersymmetry [21] and in strongly coupled theories where the light Higgs boson is considered to be a pseudo-Nambu-Goldstone boson of an underlying broken global symmetry, e.g., in little Higgs models [22] and in models with partial compositeness [8, 23, 24]. VLQ dynamics may also be an important ingredient of the physics that underlies flavor and CP-violation [9, 11, 13–15, 19, 25].

In particular, in the VLQ case depicted in diagram (a) of Fig. 1, two types of SU(2) VLQ multiplets are required in order to generate the effective operators of Eq. 1: $(F_1, F_2) = (\text{doublet, singlet})$ and/or $(F_1, F_2) = (\text{doublet, triplet})$. We will adopt a SM-like (doublet, singlet) VLQ setup, assuming three generations of SU(2) VLQ doublets $Q_i = (U, D)_i$ and the corresponding up-type and down-type SU(2) singlets U_i and D_i , respectively, carrying the same quantum numbers as the SM quarks doublets and singlets: $Q = (3, 2, 1/6)$, $U = (3, 1, 2/3)$ and $D = (3, 1, -1/3)$. We assume that the VLQ are in their mass basis, having explicit mass terms in the full Lagrangian, i.e., $M_F(\bar{F}_L F_R + \bar{F}_R F_L)$, with a mass $M_{F=Q,U,D} \sim 1 - 2$ TeV (the typical lower bounds on the masses of new VLQ states are in the range 1-1.5 TeV, depending on their mixing with the SM quarks and on their decay pattern [26]). These VLQ will also have in general the following Yukawa-like couplings to the SM Higgs (which upon EWSB also give a small contribution to their masses):

$$-\mathcal{L}_V^Y = \hat{\lambda}_{QU} \bar{Q}_L \tilde{\phi} U_R + \hat{\lambda}_{QD} \bar{Q}_L \phi D_R + h.c., \quad (11)$$

where $\hat{\lambda}_{QU}$ and $\hat{\lambda}_{QD}$ are 3×3 matrices in the VLQ flavor space in their mass basis (we have suppressed the generation index of the VLQ).

The Yukawa-like mixing terms of the VLQ with the SM quarks are in general:^[2]

$$\begin{aligned} -\mathcal{L}_{Vq}^Y = & \hat{\lambda}_{Uq} \bar{q}_L \tilde{\phi} U_R + \hat{\lambda}_{Dq} \bar{q}_L \phi D_R, \\ & + \hat{\lambda}_{Qu} \bar{Q}_L \tilde{\phi} u_R + \hat{\lambda}_{Qd} \bar{Q}_L \phi d_R + h.c. \end{aligned} \quad (12)$$

where, here also, $\hat{\lambda}_{Uq, Dq, Qu, Qd}$ are all 3×3 matrices in the VLQ - SM quarks flavor space and the SM quark fields are also assumed to be in their physical mass basis.

With this setup, diagram (a) in Fig. 1 generates the following 3×3 Wilson coefficients/matrices $\hat{f}_{uH}, \hat{f}_{dH}$ (i.e.,

[2] With the VLQ setup presented here the CKM matrix is extended and the SM 3×3 CKM block is, in principle, no longer unitary. However, the deviations from unitarity are expected to be $\propto m_q^2/m_{VLQ}^2$ and, therefore, very small for $m_q \leq m_b$ and $m_{VLQ} \gtrsim 1$ TeV, see e.g., [9]. The details of such deviations of the SM 3×3 CKM block from unitarity depend on the flavor structure of the underlying UV completion which contains the heavy VLQ fields and is beyond the scope of this work.

Z_3 symmetry 1: $\alpha(q_L^k) = \alpha(u_R^k) = \alpha(d_R^k) = (1, 2, 3)$, $\alpha(Q_L^k) = \alpha(D_R^k) = (1, 2, 0)$, $\alpha(U_R^k) = (1, 2, 1)$
$\hat{Y}_d, \hat{Y}_u, \hat{\lambda}_{QD} \in \begin{pmatrix} \times & 0 & 0 \\ 0 & \times & 0 \\ 0 & 0 & \times \end{pmatrix} \quad \hat{\lambda}_{QU}, \hat{\lambda}_{Uq} \in \begin{pmatrix} \times & 0 & \times \\ 0 & \times & 0 \\ 0 & 0 & 0 \end{pmatrix} \quad \hat{\lambda}_{Qd}, \hat{\lambda}_{Qu}, \hat{\lambda}_{Dq} \in \begin{pmatrix} \times & 0 & 0 \\ 0 & \times & 0 \\ 0 & 0 & 0 \end{pmatrix}$
$\hat{f}_{dH}, \hat{f}_{uH} \in \begin{pmatrix} \times & 0 & 0 \\ 0 & \times & 0 \\ 0 & 0 & 0 \end{pmatrix}$
Z_3 symmetry 2: $\alpha(q_L^k) = \alpha(u_R^k) = \alpha(d_R^k) = (1, 2, 3)$, $\alpha(Q_L^k) = \alpha(U_R^k) = (1, 2, 1)$, $\alpha(D_R^k) = (1, 2, 0)$
$\hat{Y}_d, \hat{Y}_u \in \begin{pmatrix} \times & 0 & 0 \\ 0 & \times & 0 \\ 0 & 0 & \times \end{pmatrix} \quad \hat{\lambda}_{QD}, \hat{\lambda}_{Qu}, \hat{\lambda}_{Qd} \in \begin{pmatrix} \times & 0 & 0 \\ 0 & \times & 0 \\ \times & 0 & 0 \end{pmatrix} \quad \hat{\lambda}_{QU} \in \begin{pmatrix} \times & 0 & \times \\ 0 & \times & 0 \\ \times & 0 & \times \end{pmatrix} \quad \hat{\lambda}_{Uq} \in \begin{pmatrix} \times & 0 & \times \\ 0 & \times & 0 \\ 0 & 0 & 0 \end{pmatrix} \quad \hat{\lambda}_{Dq} \in \begin{pmatrix} \times & 0 & 0 \\ 0 & \times & 0 \\ 0 & 0 & 0 \end{pmatrix}$
$\hat{f}_{dH}, \hat{f}_{uH} \in \begin{pmatrix} \times & 0 & 0 \\ 0 & \times & 0 \\ 0 & 0 & 0 \end{pmatrix}$
Z_3 symmetry 3: $\alpha(q_L^k) = \alpha(d_R^k) = (1, 2, 3)$, $\alpha(Q_L^k) = \alpha(U_R^k) = \alpha(u_L^k) = (1, 2, 1)$, $\alpha(D_R^k) = (1, 2, 0)$
$\hat{Y}_d, \hat{\lambda}_{Dq} \in \begin{pmatrix} \times & 0 & 0 \\ 0 & \times & 0 \\ 0 & 0 & \times \end{pmatrix} \quad \hat{Y}_u, \hat{\lambda}_{Uq} \in \begin{pmatrix} \times & 0 & \times \\ 0 & \times & 0 \\ 0 & 0 & 0 \end{pmatrix} \quad \hat{\lambda}_{QD}, \hat{\lambda}_{Qd} \in \begin{pmatrix} \times & 0 & 0 \\ 0 & \times & 0 \\ \times & 0 & 0 \end{pmatrix} \quad \hat{\lambda}_{QU}, \hat{\lambda}_{Qu} \in \begin{pmatrix} \times & 0 & \times \\ 0 & \times & 0 \\ \times & 0 & \times \end{pmatrix}$
$\hat{f}_{dH} \in \begin{pmatrix} \times & 0 & 0 \\ 0 & \times & 0 \\ 0 & 0 & 0 \end{pmatrix} \quad \hat{f}_{uH} \in \begin{pmatrix} \times & 0 & \times \\ 0 & \times & 0 \\ 0 & 0 & 0 \end{pmatrix}$

TABLE I: Flavor textures for the fermions Yukawa-like couplings $\hat{Y}_{u,d}$, $\hat{\lambda}_{QU, QD, Qu, Qd, Uq, Dq}$ and the corresponding Wilson coefficients $\hat{f}_{uH} = \hat{\lambda}_{Uq} \hat{\lambda}_{QU}^\dagger \hat{\lambda}_{Qu}$ and $\hat{f}_{dH} = \hat{\lambda}_{Dq} \hat{\lambda}_{QD}^\dagger \hat{\lambda}_{Qd}$, assuming three different Z_3 symmetries due to three types of Z_3 charge assignments for the fermion fields in their mass basis. Our notation for the charge assignments is $\alpha(\psi^k) = (a, b, c)$, using k as the generation index, so that $\alpha(\psi^1) = a$, $\alpha(\psi^2) = b$ and $\alpha(\psi^3) = c$. See also text.

in the physical quark mass basis) and effective scales of the operators in Eq. 1:

$$\hat{f}_{uH} = \hat{\lambda}_{Uq} \hat{\lambda}_{QU}^\dagger \hat{\lambda}_{Qu} \quad , \quad \Lambda = \sqrt{M_U M_Q} \quad , \quad (13)$$

$$\hat{f}_{dH} = \hat{\lambda}_{Dq} \hat{\lambda}_{QD}^\dagger \hat{\lambda}_{Qd} \quad , \quad \Lambda = \sqrt{M_D M_Q} \quad . \quad (14)$$

Thus, if the VLQ have a mass $M \sim M_U \sim M_D \sim M_Q \sim 1.5$ TeV and natural couplings $\hat{\lambda}_i \sim \mathcal{O}(1)$ (so that $\hat{f}_{qH}^{ij} \sim \mathcal{O}(1)$), then the Yukawa couplings of all light quarks are universally enhanced, with a typical size of (see Eq. 5):

$$y_u^{ij} \sim \frac{v^2}{M^2} \left(\hat{\lambda}_{Uq} \hat{\lambda}_{QU}^\dagger \hat{\lambda}_{Qu} \right)^{ij} \xrightarrow[M \sim 1.5 \text{ TeV}]{\hat{\lambda}_k^{ij} \sim \mathcal{O}(1)} y_b^{SM} \quad , \quad (15)$$

$$y_d^{ij} \sim \frac{v^2}{M^2} \left(\hat{\lambda}_{Dq} \hat{\lambda}_{QD}^\dagger \hat{\lambda}_{Qd} \right)^{ij} \xrightarrow[M \sim 1.5 \text{ TeV}]{\hat{\lambda}_k^{ij} \sim \mathcal{O}(1)} y_b^{SM} \quad . \quad (16)$$

Therefore, depending on the structure of the VLQ Yukawa-like couplings $\hat{\lambda}_k$, potentially “dangerous” FCNC $q_i q_j h$ transitions of the same size may also be generated, i.e., $y_q^{ij} \sim \mathcal{O}(y_b^{SM})$ for $i \neq j$.

Indeed, FCNC in the down quark sector and among the 1st and 2nd generations of the up quark sector

are severely constrained by experiment - to the level of $y_d^{12,21} \lesssim 10^{-5}$, $y_d^{13,31,23,32} \lesssim 10^{-4}$, $y_u^{12,21} \lesssim 10^{-5}$ [27]. This puts stringent constraints on the off-diagonal elements of the Wilson coefficients \hat{f}_{qH} . In particular, for $\Lambda \sim \mathcal{O}(1)$ TeV, these bounds correspond to $\hat{f}_{dH}^{ij} \lesssim 10^{-3} - 10^{-4}$ for $i \neq j$ and $\hat{f}_{uH}^{12,21} \lesssim 10^{-4}$, which therefore constrain the corresponding flavor changing VLQ coupling to the SM quarks. This observed smallness of FCNC $q_i \rightarrow q_j$ transitions is a strong indication that any viable underlying UV completion of the SM, and in particular of the above VLQ scenario, should have a mechanism which strongly suppresses or forbids the above Higgs mediated FC couplings. Such a mechanism is often assumed to be linked to an underlying flavor symmetry which gives flavor selection rules, thus imposing specific flavor textures on the FCNC couplings.

There are several types of mechanisms and/or flavor symmetries that can be applied to our VLQ framework, that will give the desired flavor selection rules. Here we wish to consider simple and rather minimal examples of flavor symmetries which are consistent with both the current experimental constraints on FCNC and with our UEHiggsY framework. In particular, we introduce a Z_3 flavor symmetry under which the physical states

(i.e., mass eigenstates) of the SM quarks and VLQ fields transform as $\psi^k \rightarrow e^{i\alpha(\psi^k)\tau_3} \psi^k$, where $\tau_3 \equiv 2\pi/3$, k is the generation index, $\psi = q_L, u_R, d_R, Q_L, U_R, D_R$ and $\alpha(\psi^k)$ are the Z_3 charges of ψ^k .

The simplest Z_3 setup, which has no tree-level FCNC and also accommodates the UEHiggsY paradigm is the choice $\alpha(\psi^k) = k$. In this case, all the Yukawa-like couplings involving the VLQ, i.e., $\hat{\lambda}_i$ in Eqs. 11 and 12 as well as the SM Yukawa couplings $\hat{Y}_{u,d}$ are diagonal, so that the Wilson coefficients \hat{f}_{uH} and \hat{f}_{dH} are also diagonal, giving $y_q^{ij} \sim y_b^{SM} \delta_{ij}$ for $q = u, d, c, s, b$ and no tree-level FCNC. In particular, with the Z_3 symmetry $\alpha(\psi_k) = k$, the UEHiggsY setup of Eqs. 9 and 10 is realized with only diagonal entries of \hat{Y}_q and \hat{f}_{qH} :

$$\hat{Y}_q^{ii} = -\frac{y_b^{SM}}{\sqrt{2}} \left(1 - \frac{3}{\sqrt{2}} \frac{m_{q_i}}{m_b} \right), \quad (17)$$

$$\hat{f}_{qH}^{ii} = -\frac{\sqrt{2}y_b^{SM}}{\epsilon} \left(1 - \frac{1}{\sqrt{2}} \frac{m_{q_i}}{m_b} \right). \quad (18)$$

In Table I we list three additional examples of Z_3 symmetries which correspond to different charge assignments to the fermion fields and yield non-diagonal structures (textures) for some of the Yukawa-like couplings and Wilson coefficients. In particular, with the Z_3 symmetries 1 and 2 the SM Yukawa couplings $\hat{Y}_{u,d}$ as well as Wilson coefficients $\hat{f}_{uH,dH}$ are diagonal and $f_{uH,dH}^{33} = 0$. Thus, these two flavor symmetries with the $Y_{u,d}^{11,22}$ and $\hat{f}_{uH,dH}^{11,22}$ entries of Eqs. 17 and 18 and with $Y_u^{33} = \sqrt{2}m_t/v$ and $Y_d^{33} = \sqrt{2}m_b/v$, will bring about the UEHiggsY scenario with no tree-level FCNC.

The third Z_3 symmetry in Table I generates a tree-level $\bar{u}_L t_R h$ FCNC coupling (due to $\hat{f}_{uH}^{13} \neq 0$), which is not well constrained and which may yield an interesting signal of exclusive production of the Higgs boson in association with a single top-quark at the LHC. This effect will be discussed in more detail in section V D. Notice also that, while the flavor structures of the SM Yukawa coupling and Wilson coefficients in the down-quark sector are similar in all the three Z_3 symmetries, the up-quark sector corresponding to the third Z_3 symmetry has a rank 2 mass matrix, requiring $\epsilon \hat{f}_{uH}^{13} = 2\hat{Y}_u^{13}$ in order to have a diagonal up-quark mass matrix (i.e., $M_u^{13} = 0$). Thus, in this case there are only two non-zero mass eigenvalues in the up-quark sector, so that the UV completion of the VLQ scenario should have another mechanism for generating the top-quark mass, e.g., by coupling the top-quark to another scalar doublet.

IV. CONSTRAINTS FROM THE 125 GEV HIGGS SIGNALS

The measured signals of the 125 GeV Higgs-like particle are sensitive to a variety of new physics scenarios, which may alter the Higgs couplings to the known SM

particles involved in its production and decay channels. In particular, modifications of the Higgs Yukawa couplings to the light fermions may lead in general to deviations in both Higgs production and decays.

To see that, we will use the Higgs “signal strength” parameters, which are defined as the ratio between the Higgs production and decay rates and their SM expectations:

$$\mu_i^f = \frac{\sigma(i \rightarrow h \rightarrow f)}{\sigma(i \rightarrow h \rightarrow f)_{SM}} \equiv \mu_i \cdot \mu^f, \quad (19)$$

with (in the narrow Higgs width approximation):

$$\mu_i = \frac{\sigma(i \rightarrow h)}{\sigma(i \rightarrow h)_{SM}}, \quad (20)$$

$$\mu^f = \frac{\Gamma(h \rightarrow f)/\Gamma^h}{\Gamma(h \rightarrow f)_{SM}/\Gamma_{SM}^h}, \quad (21)$$

where $\Gamma^h(\Gamma_{SM}^h)$ are the total width of the 125 GeV Higgs(SM Higgs), i represents the parton content in the proton which is involved the production mechanism and f is the Higgs decay final state.

We will consider the signal strength parameters associated with the production processes $pp \rightarrow h$ and $pp \rightarrow hW, hZ$ followed by the decays $h \rightarrow \gamma\gamma, WW^*, ZZ^*, \tau\tau$ and $h \rightarrow bb$, as analysed by the ATLAS and CMS collaborations [28].^[3] In the SM, the s-channel production of the 125 GeV Higgs is dominated by the gluon-fusion production mechanism $gg \rightarrow h$. In particular, the SM tree-level $q\bar{q}$ -fusion production channel, $q\bar{q} \rightarrow h$, is negligible due to the vanishingly small light-quarks SM Yukawa couplings (the effect of the light quarks in the 1-loop ggh coupling is also negligible for our purpose, i.e., about $\sim 7\%$ (LO) for the b-quark [6, 28–30]). In the $pp \rightarrow Vh$ channels ($V = W, Z$), the SM rate is dominated by the s-channel V exchange $q\bar{q} \rightarrow V^* \rightarrow Vh$.

A different picture arises in our UEHiggsY framework, where the Higgs Yukawa couplings to all the light-quarks ($q = u, d, c, s$) are universally modified/enhanced. Higgs production via $q\bar{q}$ -fusion becomes important, in particular, the tree-level processes $q\bar{q} \rightarrow h$ and t-channel Vh production $q\bar{q} \rightarrow Vh$ (see diagram for $q\bar{q} \rightarrow \gamma h$ in Fig. 2 and replace $\gamma \rightarrow V$, $V = Z$ or W). To study the effect of these new $q\bar{q}$ -fusion Higgs production channels, we define Yukawa coupling modifiers, κ_q , and scale them with the SM b-quark Yukawa, as follows:

$$\kappa_q \equiv \frac{y_q}{y_b^{SM}}, \quad (22)$$

so that, in the SM, we have $\kappa_b = 1$, $\kappa_c \sim 0.3$, $\kappa_s \sim \mathcal{O}(10^{-2})$ and $\kappa_{u,d} \sim \mathcal{O}(10^{-3})$. On the other hand, in the

[3] We neglect Higgs production via $pp \rightarrow t\bar{t}h$, which, although included in the ATLAS and CMS fits, are 2-3 orders of magnitudes smaller than the gluon-fusion channel. Also, the vector-boson fusion (VBF) process $VV \rightarrow h$ is not relevant to our discussion below.

UEHiggsY paradigm with a NP scale $\Lambda \sim \mathcal{O}(1 \text{ TeV})$ and $\mathcal{O}(1)$ couplings of the heavy states to the SM particles, we expect $\kappa_q \sim \mathcal{O}(1)$ for all light-quarks $q = d, u, s, c$ as well as for the b -quark (see discussion below Eq. 5). In this case the tree-level $q\bar{q} \rightarrow h$ and $h \rightarrow q\bar{q}$ production and decay channels also contribute to the signal strength factors μ_i and μ^f defined in Eqs. 20 and 21. We neglect below the correction to the 1-loop $gg \rightarrow h$ Higgs production channel, which arises in our UEHiggsY setup from the light-quarks of the 1st and 2nd generations. As explained below, this correction is of the order of at most several percent, even with $y_q \sim y_b^{SM}$ for all $q = u, d, c, s$. In particular, the contribution of each light-quark (i.e., in the limit that $m_h^2 \gg m_q^2$) to the 1-loop ggh amplitude is (see e.g., [31]):

$$A_q \propto y_q \cdot \frac{m_q \cdot v}{m_h^2} \cdot \log^2 \left(\frac{m_h^2}{m_q^2} \right) , \quad (23)$$

and their leading effect to the overall 1-loop gluon-fusion Higgs production channel arises from their interference with the top-quark loop (similar to the case of the leading b -quark contribution in the SM). Thus, the relative size of any light-quark contribution to the ggh coupling with respect to that of the b -quark one is:

$$\frac{A_q}{A_b} \sim \frac{y_q}{y_b} \cdot \frac{m_q}{m_b} \cdot \frac{\log^2 \left(\frac{m_h^2}{m_q^2} \right)}{\log^2 \left(\frac{m_h^2}{m_b^2} \right)} , \quad (24)$$

so that the contribution to $gg \rightarrow h$ from a $c(s)$ -quark with $y_c(y_s) \sim y_b^{SM}$ is about 50%(20%) of the SM b -quark one, i.e., $A_c(A_s) \sim 0.5(0.2)A_b$. Furthermore, the effect of the light-quarks of the 1st generation is about a hundred times smaller than the SM b -quark one. Therefore, since the b -quark contribution to the 1-loop ggh production cross-section is less than 10% (and is included below), the overall UEHiggsY effect on the $gg \rightarrow h$ cross-section is around 5% if all the light-quarks have Yukawa couplings $y_q \sim y_b^{SM}$ and is, therefore, neglected in the analysis below.

Note that, in the decay $h \rightarrow \gamma\gamma$, the dominant contribution arises from the W -boson loop and, as a consequence, the relative effect of the light-quarks loops in our UEHiggsY scenario with $y_q \sim y_b^{SM}$ is much smaller. In particular, the top-quark loop contributes about 30% of $\Gamma(h \rightarrow \gamma\gamma)$, mostly from its interference with the W loop [28]. Thus, for example, the c -quark loop with $y_c \sim y_b^{SM}$ which is $A_c \sim 0.03A_t$ (see Eqs. 23 and 24), will be negligibly small for our purpose.

In particular, in the UEHiggsY setup we have:

$$\begin{aligned} \mu_{i=gg+q\bar{q}}^{UEHiggsY} &\approx \frac{\sigma(gg \rightarrow h)_{SM} + \hat{\sigma}(q\bar{q} \rightarrow h)_{UEHiggsY}}{\sigma(gg \rightarrow h)_{SM}} \\ &\equiv 1 + \sum_q \kappa_q^2 R_q , \end{aligned} \quad (25)$$

and

$$\mu_{UEHiggsY}^f \approx \frac{\kappa_f^2}{1 - \left(1 - \kappa_b^2 - \sum_q \kappa_q^2 \right) BR(h \rightarrow b\bar{b})_{SM}} , \quad (26)$$

where $\kappa_f = g_{hff}/g_{hff}^{SM}$ are the couplings modifiers of any of the hff Higgs decay vertices and R_q is defined by the scaled UEHiggsY $q\bar{q} \rightarrow h$ cross-section evaluated with $\kappa_q = 1$, i.e., using $\sigma(q\bar{q} \rightarrow h)_{UEHiggsY} \equiv \hat{\sigma}(q\bar{q} \rightarrow h)_{UEHiggsY}/\kappa_q^2$, as:

$$R_q \equiv \frac{\sigma(q\bar{q} \rightarrow h)_{UEHiggsY}}{\sigma(gg \rightarrow h)_{SM}} , \quad (27)$$

where it is understood that $\sigma(q\bar{q}, gg \rightarrow h)$ are convoluted with the corresponding PDF weights and that $\sigma(q\bar{q} \rightarrow h)_{UEHiggsY}$ are calculated at tree-level with the values $\kappa_q = 1$ for all light flavors $q = u, d, c, s$. Furthermore, in what follows we set the b -quark Yukawa coupling to its SM value, i.e., $\kappa_b = 1$, and neglect the $b\bar{b}$ -fusion production channel $b\bar{b} \rightarrow h$, which is much smaller than the light-quark fusion channels, $q\bar{q} \rightarrow h$, when evaluated with $\kappa_q \sim \mathcal{O}(1)$.

All cross-sections $\sigma(q\bar{q} \rightarrow h)$ are calculated using MadGraph5 [39] at LO parton-level, where a dedicated universal FeynRules output (UFO) model for the UEHiggsY framework was produced for the MadGraph5 sessions using FeynRules [40]. We used the MadGraph5 default PDF set (nn23lo1) and a dynamical scale choice for the central value of the factorization (μ_F) and renormalization (μ_R) scales corresponding to the sum of the transverse mass in the hard-process. In particular, we find $\sigma(u\bar{u}, d\bar{d}, s\bar{s}, c\bar{c} \rightarrow h)_{UEHiggsY} \approx 33.7, 23.8, 5.4, 4.0$ [pb] at the 13 TeV LHC, so that using the N3LO QCD prediction (at the 13 TeV LHC) $\sigma(gg \rightarrow h) \approx 48.6$ [pb] [37], we obtain $\sum_q R_q \sim 1.4$ and, therefore:

$$\mu_{i=gg+q\bar{q}}^{UEHiggsY} = 1 + \kappa_q^2 \sum_q R_q \sim 1 + 1.4 K_q \kappa_q^2 , \quad (28)$$

where we have added a common K-factor, K_q , to the tree-level calculated cross-sections $\sigma(q\bar{q} \rightarrow h)_{UEHiggsY}$. In particular, with $K_q \sim 1.5$ (see e.g., [38]) and the UEHiggsY values $\kappa_q = 1$ for all $q = u, d, c, s$, we find that $\mu_{i=gg+q\bar{q}}^{UEHiggsY} \sim 3$, so that the 125 GeV Higgs production mechanism is enhanced in the UEHiggsY framework by a factor of $\mathcal{O}(3)$ with respect to the SM expectation.

Turning now to the Higgs decay channels $h \rightarrow \gamma\gamma$, ZZ^* , WW^* , $b\bar{b}$, $\tau^+\tau^-$ and assuming no new physics in the decay (by setting $\kappa_f = 1$ for $f = \gamma, Z, W, b, \tau$), we obtain from Eq. 26:

$$\mu_{UEHiggsY}^{\gamma, Z, W, b, \tau} = \frac{1}{1 + 4\kappa_q^2 BR(h \rightarrow b\bar{b})_{SM}} . \quad (29)$$

Thus, under the UEHiggsY paradigm with $\kappa_q = 1$ we have $\mu_{UEHiggsY}^{\gamma, Z, W, b, \tau} \sim 0.3$, so that the calculated signal strengths of Eq. 19 in these channels are all expected to be the same:

$$\mu_{i=gg+qq}^{\gamma, Z, W, b, \tau} = \mu_{i=gg+qq}^{UEHiggsY} \cdot \mu_{i=gg+qq}^{\gamma, Z, W, b, \tau} \approx \frac{1 + 1.4 K_q \kappa_q^2}{1 + 4 \kappa_q^2 BR(h \rightarrow b\bar{b})_{SM}} \xrightarrow[\kappa_q=1]{\kappa_q=1.5} 0.93 . \quad (30)$$

Indeed, the best measured signal strengths in the four channels $pp \rightarrow h \rightarrow \gamma\gamma$, ZZ^* , WW^* , $\tau^+\tau^-$ have a typical 1σ error of 10-20% and are therefore all consistent with the value $\mu_{i=gg+qq}^{\gamma, Z, W, b, \tau} \sim 0.93$ within $1 - 2\sigma$ (for the LHC RUN1 results see [28] and for updated results from RUN2 see e.g., [32]). In particular, the currently measured 125 GeV Higgs signals in these four channels do not constrain the UEHiggsY paradigm with $\kappa_q = 1$ for all $q = u, d, s, c$.

Let us next consider the UEHiggsY effect on the measured hV production channel followed by $h \rightarrow b\bar{b}$. This process has currently the best sensitivity to the $h \rightarrow b\bar{b}$ decay channel and is used to overcome the large QCD background to the simpler $pp \rightarrow h \rightarrow b\bar{b}V$ channel. In particular, in this channel we define $\mu(pp \rightarrow hV \rightarrow b\bar{b}V) \equiv R_{hV \rightarrow b\bar{b}V} = R_{hV} \cdot \mu^b$, with ($V = W, Z$):

$$R_{hV} = \frac{\sigma^{hV}}{\sigma_{SM}^{hV}} , \quad (31)$$

where $\sigma^{hW}, \sigma^{hZ} \equiv \sigma(pp \rightarrow hW^+ + hW^-), \sigma(pp \rightarrow hZ)$.

As mentioned earlier, in the UEHiggsY framework, the SM s-channel production process $q\bar{q} \rightarrow V^* \rightarrow hV$ receives additional tree-level contributions from t-channel q -exchange diagrams, similar to the one depicted for the process $q\bar{q} \rightarrow h\gamma$ in Fig. 2. In particular, calculating the contribution of these diagrams under the UEHiggsY working assumption with $\kappa_q = 1$ for all $q = u, d, c, s$, we find $R_{hV}^{UEHiggsY} \sim 1.1$ for both $V = W$ and $V = Z$. Therefore, since $\mu_{UEHiggsY}^b \sim 0.3$ for $\kappa_q = 1$ (see Eq. 29), the UEHiggsY signal strength parameter in the $pp \rightarrow Vh \rightarrow b\bar{b}V$ channel, $R_{hV \rightarrow b\bar{b}V}$, is expected to be appreciably smaller than one (i.e., than its SM value):

$$R_{hV \rightarrow b\bar{b}V} = R_{hV}^{UEHiggsY} \cdot \mu_{UEHiggsY}^b \xrightarrow[\kappa_q=1]{\kappa_q=1} 0.33 , \quad (32)$$

for both the hW and hZ production channels.

It is interesting to note that the RUN1 best fitted value for the measured signal strength in this channel, $pp \rightarrow hV \rightarrow b\bar{b}V$, was indeed on the lower side and consistent with the above predicted UEHiggsY value $R_{hV \rightarrow b\bar{b}V} \sim 0.33$ within about 1σ : the combined ATLAS and CMS analysis of RUN1 data yielded $R_{hV \rightarrow b\bar{b}V} \sim 0.65 \pm 0.3$ [28]. Recent updated ATLAS and CMS analysis in this channel, combining the RUN1 data with about 36 fb^{-1} of RUN2 data at a center of mass energy of 13 TeV yielded higher values $R_{hV \rightarrow b\bar{b}V} \sim 0.9 \pm 0.3$ [33] and $R_{hV \rightarrow b\bar{b}V} \sim 1.06 \pm 0.3$ [34], respectively, but the errors in these channels are still large.

We thus conclude that, currently, no significant constraints can be imposed on the UEHiggsY paradigm from

the measured 125 GeV Higgs signals. We also note that the Higgs Yukawa couplings to the light quarks can also effect the transverse momentum distributions in Higgs production at the LHC [4, 6, 41]. However, the errors of the current measured normalized $p_T(h)$ in Higgs + jets production are still relatively large, so that this analysis also cannot yet be used to exclude scenarios with $\kappa_q \sim \mathcal{O}(1)$ for the light quarks [4, 6] (see also discussion in the next section).

V. HIGGS SIGNALS OF THE UEHIGGSY PARADIGM

Enhanced light-quark Yukawa couplings may have direct consequences in Higgs production and decay phenomenology at the LHC. Indeed, one good example that was discussed in the previous section is $pp \rightarrow Vh$ followed by the Higgs decay $h \rightarrow b\bar{b}$, which may be sensitive to the UEHiggsY paradigm with improved precision in the measurement of this Higgs production and decay channel. Here, we wish to discuss at the exploratory level some of the “smoking gun” signals of the UEHiggsY paradigm, associated with the higher dimension effective operators of Eq. 1.

Let us define the normalized cross-section ratios:

$$R_{F(h)} \equiv \frac{\sigma(pp \rightarrow F(h))}{\sigma(pp \rightarrow F(h))_{SM}} , \quad (33)$$

where $F(h)$ stands for a final state with at least one Higgs. In particular, apart from the $pp \rightarrow h, hV$ Higgs production channels discussed in the previous section, the UEHiggsY framework potentially effects other processes which involve one or more Higgs particles in the final state. Below we will consider some of the Higgs final states which have a noticeable tree-level sensitivity to the UEHiggsY paradigm and which are also recognized, in general, as sensitive probes of NP [42]: Higgs pair and triple Higgs productions, Higgs + jets production, Higgs + single top associated production and Higgs production with a single photon, i.e., $F(h) = hh, hhh, h + nj, ht, h\gamma$.^[4]

Here also, all cross-sections are calculated at LO parton level, using MadGraph5_{aMC}@NLO [39], with default PDF set and dynamical scale choice for the central value

[4] Some of the Higgs signals considered in this section may also be sensitive at 1-loop to modifications of the 3rd generation Yukawa couplings due to the effective operators in Eq. 1, see e.g., [43–46].

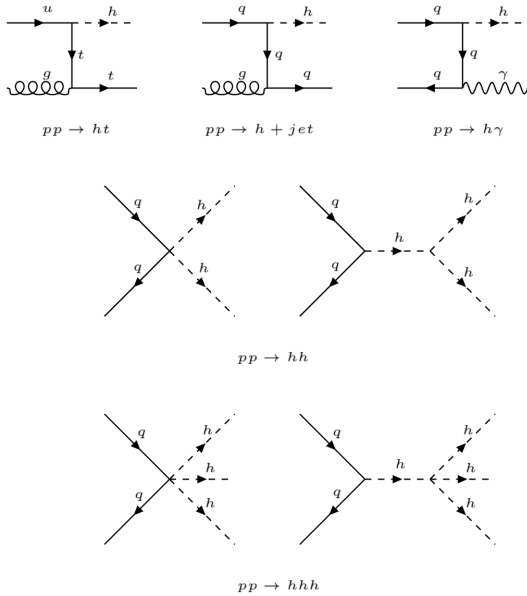


FIG. 2: Sample diagrams for the processes $pp \rightarrow hh$, hhh , $h+jet$, ht , $h\gamma$ due to enhanced qqh couplings within the UEHiggsY paradigm.

of the factorization and renormalization scales. In addition, following the working assumption of the UEHiggsY paradigm, the effective operators in Eq. 1 are assumed to have a typical scale of $\Lambda \sim \mathcal{O}(1)$ TeV and couplings $f_{qH} \sim \mathcal{O}(1)$, so that all cross-sections reported below are calculated with qqh Yukawa couplings comparable to the SM b-quark Yukawa, i.e., $y_q \sim y_b^{SM}$.

A. Multi-Higgs production $pp \rightarrow hh$, hhh

Higgs pair production is one of the main targets for NP searches in the Higgs sector at the LHC, primarily due to its sensitivity to the Higgs self coupling in the Higgs potential and to heavy NP in the loop induced couplings of the Higgs to gluons [16, 35]. In the SM this process is initiated at LO by 1-loop gluon-fusion diagrams $gg \rightarrow hh$, and the corresponding cross-section is $\sigma(pp \rightarrow hh) \sim 15$ fb at LO, where due to the large QCD corrections, it is typically doubled at NLO [36].

In the UEHiggsY framework, there are additional tree-level diagrams induced by the effective operators of Eq. 1, as depicted in Fig. 2. Setting $\hat{f}_{qH}^{ij} = \delta_{ij}$ (i.e., assuming only flavor diagonal couplings) and $\Lambda \sim \mathcal{O}(1)$ TeV, we have $y_q \sim y_b^{SM}$ for the qqh Yukawa coupling (see Eq. 5) and $\Gamma_{hh}^{qq} \sim 3y_b^{SM}/v$ for the qqh couplings (see Eq. 6). For this setup we find at LO and for the 13 TeV LHC:

$$R_{hh} \equiv \frac{\sigma(pp \rightarrow hh)}{\sigma(pp \rightarrow hh)_{SM}} \sim 100, \quad (34)$$

where more than 90% of the enhancement arises from

the tree-level diagrams initiated by the u and d quarks. In particular, the total Higgs production cross-section within the UEHiggsY framework with $y_q \sim y_b^{SM}$ for $q = u, d, c, s, b$ is $\sigma(pp \rightarrow hh) \sim 1.5$ pb.

The current best bounds on the hh production cross-section at the 13 TeV are $R_{hh \rightarrow b\bar{b}\gamma\gamma} \lesssim 19$ in the $hh \rightarrow b\bar{b}\gamma\gamma$ decay channel (obtained by the CMS collaboration, see [47]) and $R_{hh \rightarrow b\bar{b}b\bar{b}} \lesssim 29$ in the $hh \rightarrow b\bar{b}b\bar{b}$ decay channel (obtained by the ATLAS collaboration, see [48]).

As was shown in the previous section, in our UEHiggsY framework with $\hat{f}_{qH}^{ij} = \delta_{ij}$ and $\Lambda \sim \mathcal{O}(1)$ TeV (for which $y_q \sim y_b^{SM}$ for $q = u, d, c, s, b$) the branching ratios for the decays $h \rightarrow bb$ and $h \rightarrow \gamma\gamma$ are decreased by about a factor of three with respect to the SM: $BR(h \rightarrow bb, \gamma\gamma) \sim 0.3BR(h \rightarrow b\bar{b}, \gamma\gamma)_{SM}$ (see Eq. 29 with $\kappa_q = 1$). Therefore, in these channels we obtain in the UEHiggsY framework: $R_{hh \rightarrow b\bar{b}b\bar{b}} = R_{hh \rightarrow b\bar{b}\gamma\gamma} \sim 100 \times (0.3)^2 \sim 10$, which is an order of magnitude larger than the SM rate, but still below the current sensitivity.

For the triple Higgs production channel, $pp \rightarrow hhh$, the SM cross-section is around $\sigma(pp \rightarrow hhh) \sim 30$ ab at LO and about twice larger at NLO [42]. In the UEHiggsY framework (see representative diagrams in Fig. 2) we find that $\sigma(pp \rightarrow hhh) \sim 10$ [fb], so that:

$$R_{hhh} \equiv \frac{\sigma(pp \rightarrow hhh)}{\sigma(pp \rightarrow hhh)_{SM}} \sim 300. \quad (35)$$

Thus, the expected enhancement over the SM signal in the $hhh \rightarrow b\bar{b}b\bar{b}b\bar{b}$ decay channel is again $R_{hhh \rightarrow b\bar{b}b\bar{b}b\bar{b}} \sim \mathcal{O}(10)$. However, since in the UEHiggsY case we have $BR(h \rightarrow b\bar{b}) \sim 0.18$, the triple Higgs cross-section in this channels is $\sigma(pp \rightarrow hhh \rightarrow b\bar{b}b\bar{b}b\bar{b}) \sim 10 \text{ fb} \cdot 0.18^3 \sim 60$ [ab] and, therefore, might be difficult to detect even at the HL-LHC with a luminosity of 3000 fb^{-1} .

B. Higgs + high p_T light-jet production $pp \rightarrow h+j$

In general, there is a tree-level SM contribution to the exclusive Higgs + light-jet production, $pp \rightarrow h+j$, from the hard processes $gq \rightarrow hq$, $g\bar{q} \rightarrow h\bar{q}$ and $q\bar{q} \rightarrow hg$, where $q = u, d, c$ or s . However, since the corresponding tree-level diagrams (see e.g., the t-channel diagram for $gq \rightarrow hq$ in Fig. 2) are proportional to the light-quarks Yukawa couplings, the effect of these light-quark initiated hard-processes on the overall $pp \rightarrow h+j$ cross-section is negligibly small in the SM (i.e., when $y_q \ll 1$ in particular for $q = u, d$). Thus, the dominant SM contribution to the Higgs + light-jet cross-section arises from the 1-loop gluon-fusion process $gg \rightarrow gh$, which, at leading order, is generated mainly by 1-loop top-quark exchanges.

If, on the other hand, $y_q \sim y_b^{SM}$ for all $q = u, d, c, s$, as expected in the UEHiggsY framework, then the contribution (to the $pp \rightarrow h+j$ cross-section) from the quark initiated tree-level process $gq \rightarrow hq$, $g\bar{q} \rightarrow h\bar{q}$ and $q\bar{q} \rightarrow hg$ becomes appreciably larger. Indeed, in [41] we have

shown that the Higgs p_T distribution in $pp \rightarrow h j$ production at the LHC is a rather sensitive probe of the light-quarks Yukawa couplings (and also of other forms of NP in the Higgs-gluon hgg and quark-gluon qgg interactions) and thus of the UEHiggsY paradigm.

In particular, we have defined in [41] the signal strength for $pp \rightarrow h j$, followed by the Higgs decay $h \rightarrow f f$, where f can be any of the SM Higgs decay products (e.g., $f = b, \tau, \gamma, W, Z$):

$$\begin{aligned} R_{hj \rightarrow f\bar{f}j} &= \frac{\hat{\sigma}(pp \rightarrow h j \rightarrow f\bar{f} + j)}{\hat{\sigma}(pp \rightarrow h j \rightarrow f\bar{f} + j)_{SM}} \\ &\simeq \frac{\hat{\sigma}(pp \rightarrow h j)}{\hat{\sigma}(pp \rightarrow h j)_{SM}} \cdot \frac{BR(h \rightarrow f\bar{f})}{BR(h \rightarrow f\bar{f})_{SM}} , \end{aligned} \quad (36)$$

where $\hat{\sigma}$ is the p_T -dependent “cumulative cross-section”, satisfying a given lower Higgs p_T cut:

$$\hat{\sigma} \equiv \sigma(p_T(h) > p_T^{cut}) = \int_{p_T(h) \geq p_T^{cut}} dp_T \frac{d\sigma}{dp_T} , \quad (37)$$

and found that, in a NP scenario where $y_q \sim y_b^{SM}$ for all $q = u, d, c, s$ (which corresponds to the UEHiggsY framework discussed here), the above signal strength is significantly smaller than its SM value at the large $p_T(h)$ regime:

$$R_{hj \rightarrow f\bar{f}j} \sim 0.3 - 0.4 , \quad (38)$$

for $f = b, \tau, \gamma, W, Z$ and with a $p_T(h)$ cut in the range $p_T^{cut} \sim 200 - 1000$ GeV.

C. Higgs-photon associated production $pp \rightarrow h\gamma$

In the SM, the leading contribution to the exclusive $pp \rightarrow h\gamma$ production channel is the tree-level t-channel hard processes $c\bar{c}, b\bar{b} \rightarrow h\gamma$ (shown by the diagram for $q\bar{q} \rightarrow h\gamma$ in Fig. 2 with $q = c, b$), which give a rather small cross-section of $\sigma(pp \rightarrow h\gamma) \sim \mathcal{O}(0.1)$ [fb] with a 30 GeV $p_T(\gamma)$ -cut at the 13 TeV LHC [49, 50]. The 1-loop SM (EW) diagrams contributing to the light-quark annihilation channels, e.g., $u\bar{u}, d\bar{d} \rightarrow h\gamma$, are more than an order of magnitude smaller than the tree-level $b\bar{b}$ -fusion production channel [49] and the amplitude for the gluon-fusion production channel $gg \rightarrow h\gamma$ vanishes due to Furry’s theorem.

The SM cross-sections for inclusive $h\gamma$ production channels, such as $pp \rightarrow h\gamma + j, h\gamma + V (V = W, Z), h\gamma + t\bar{t}, h\gamma + t\bar{b}$ are of $\mathcal{O}(1)$ [fb] at the 13 TeV, whereas the SM cross-section for the inclusive VBF $h\gamma$ production channel $pp \rightarrow h\gamma + 2j$ can reach ~ 20 [fb] [50, 51].

In our UEHiggsY framework, the exclusive channel $pp \rightarrow h\gamma$ has an appreciably larger rate due to the tree-level (t-channel) light-quark fusion diagrams $q\bar{q} \rightarrow h\gamma$ shown in Fig. 2 (i.e., with $q = u, d, s, c$), which are enhanced by the $\mathcal{O}(y_b^{SM})$ qqh Yukawa couplings. In particular, setting again $f_{qH}^{ij} = \delta_{ij}$ and $\Lambda = 1.5$ TeV (leading

to $y_q \sim y_b^{SM}$), we get $\sigma(pp \rightarrow h\gamma) \sim 1250$ [fb], at the 13 TeV LHC and with $p_T(\gamma) > 30$ GeV. Thus, for the exclusive $pp \rightarrow h\gamma$ production channel we find:

$$R_{h\gamma} \equiv \frac{\sigma(pp \rightarrow h\gamma)}{\sigma(pp \rightarrow h\gamma)_{SM}} \sim 1000 , \quad (39)$$

where about 80% of the enhancement arises from the tree-level $u\bar{u}$ -fusion diagrams.

Here also, taking into account the subsequent Higgs decay, e.g., $h \rightarrow b\bar{b}, \tau^+\tau^-, \gamma\gamma$, we have $R_{h\gamma \rightarrow b\bar{b}\gamma} = R_{h\gamma \rightarrow \tau^+\tau^-\gamma} = R_{h\gamma \rightarrow \gamma\gamma\gamma} \sim 1000 \times 0.3 \sim 300$, since the UEHiggsY paradigm only effects the Higgs Yukawa couplings to the light quarks.

We note that the exclusive $pp \rightarrow h\gamma$ channel is potentially sensitive to other variants of underlying NP which can be parameterized by different forms of higher dimensional effective operators, i.e., other than the ones associated with the UEHiggsY paradigm in Eq. 1, [52]. In particular, [52] finds that $\sigma(pp \rightarrow h\gamma) \sim \mathcal{O}(10)$ [fb] can be realized by other types of NP with a typical scale of $\Lambda \sim 1$ TeV and Wilson coefficients of $\mathcal{O}(1)$. This is more than an order of magnitude smaller than the effect expected in the UEHiggsY case.

Clearly, differential distributions (e.g., such as the photon transverse momentum distribution [52]) may provide extra handles for disentangling the various types of NP that can effect the $h\gamma$ production channel at the LHC. This is, however, beyond the scope of this work.

D. Higgs-single top associated production $pp \rightarrow th$

The main SM production channels of a Higgs boson in association with a single top quark at hadron colliders are inclusive and have, at LO, two distinguishable underlying hard processes. These include an extra quark/jet accompanying the ht in the final state [42].^[5] The dominant t-channel process which is initiated by bW -fusion, $bW \rightarrow ht + j$, where the extra jet accompanies the virtual space-like W -boson, and the s-channel qq' -fusion hard-process with a virtual time-like W -boson, $qq' \rightarrow W^* \rightarrow th + j_b$, where q, q' are light quarks (i.e., primarily u, d and c, s) and j_b is a b-quark jet. The t-channel process is very sensitive to the magnitude and sign of the tth Yukawa coupling [53], and at LO in the SM has a cross-section of $\sigma(pp \rightarrow ht + j)_{SM} \sim 75$ [fb]. The cross-section for the s-channel process, $pp \rightarrow ht + j_b$, is about 25 times smaller [42].

The exclusive th production channels, $pp \rightarrow ht$ and $pp \rightarrow h\bar{t}$, involve in the SM the extremely small 1-loop FC tuh and/or tch vertices and are, therefore, negligibly small with no observable consequences [54]. On the other

[5] Another sub-leading single top production channel in the SM is the associated production of th with an on-shell W boson in the final state, $pp \rightarrow thW$.

hand, in the UEHiggsY framework we have for the FC tuh coupling (assuming for simplicity that $\hat{f}_{uH}^{13} = \hat{f}_{uH}^{31}$):

$$\mathcal{L}_{tuh} = \xi_{tu} \bar{t}uh + h.c. , \quad \xi_{tu} = \frac{\epsilon}{\sqrt{2}} \hat{f}_{uH}^{13} , \quad (40)$$

and similarly for the tch coupling, where $\epsilon = v^2/\Lambda^2$. Thus, with $\Lambda \sim 1.5$ TeV and natural underlying NP (i.e., $\hat{f}_{uH}^{13} \sim \mathcal{O}(1)$), we expect the UEHiggsY FC tuh and tch couplings to be typically of the size of the SM b-quark Yukawa coupling, $\xi_{tu,tc} \sim y_b^{SM}$, in which case the exclusive channel $pp \rightarrow th$ has a rate many orders of magnitudes larger than the SM rate, due to the tree-level $ug(cg)$ -fusion FC diagrams $u(c)g \rightarrow th$ (see Fig. 2).

In particular, setting the UEHiggsY values $\xi_{tu} = \xi_{tc} = y_b^{SM} \sim 0.02$, we get for the 13 TeV LHC: $\sigma(pp \rightarrow th(\bar{t}h)) \sim 100(20)$ [fb], with more than 90%(65%) coming from the ug -fusion hard-process (i.e., from ξ_{tu}).

Defining here the ratios:

$$R_{th/thj} \equiv \frac{\sigma(pp \rightarrow th)}{\sigma(pp \rightarrow th + j)_{SM}} , \quad (41)$$

$$\bar{R}_{\bar{t}h/\bar{t}hj} \equiv \frac{\sigma(pp \rightarrow \bar{t}h)}{\sigma(pp \rightarrow \bar{t}h + j)_{SM}} , \quad (42)$$

we find $R_{th/thj}, \bar{R}_{\bar{t}h/\bar{t}hj} \rightarrow 0$ in the SM, while $R_{th/thj} \sim 2$ and $\bar{R}_{\bar{t}h/\bar{t}hj} \sim 0.8$ in the UEHiggsY case. Notice also that the asymmetric production of th versus $\bar{t}h$ in the UEHiggsY framework is different than the corresponding asymmetry in the SM channels thj and $\bar{t}hj$. In particular, while in the UEHiggsY case the th production rate is about 5 times larger than the $\bar{t}h$ rate, in the SM the thj production rate is less than 2 times larger than the $\bar{t}hj$ rate (see [42]).

Indeed, the CMS collaboration has recently performed a dedicated search for the exclusive FC single top - Higgs associated production channel $pp \rightarrow th$ at the 13 TeV LHC with a data sample of 35.9 fb^{-1} [55]. No significant deviation from the predicted background was observed and bounds on the FC couplings ξ_{tu} and/or ξ_{tc} were obtained. In particular, the bounds were reported on the branching ratios of the corresponding FC decay channels $t \rightarrow uh, ch$, which, when translated to the FC couplings (see derivation below), give $\xi_{tu}, \xi_{tc} \lesssim 0.09$. This bound is more than 4 times larger than the expected strength of these FC couplings in the UEHiggsY framework with which the above values for $R_{th/thj}$ and $\bar{R}_{\bar{t}h/\bar{t}hj}$ were obtained (recall that, within the UEHiggs paradigm, we expect $\xi_{tu}, \xi_{tc} \sim y_b^{SM} \sim 0.02$). In other words, the current reported sensitivity to the exclusive th final state is $\sigma(pp \rightarrow th + \bar{t}h) \lesssim 16 \times \sigma(pp \rightarrow th + \bar{t}h)_{UEHiggsY}$, since the corresponding UEHiggsY predicted cross-section scales as $\xi_{tu,tc}^2$.

Finally, we note that the current best direct bounds on ξ_{tu} and ξ_{tc} were obtained by the ATLAS collaboration, which analysed the FC top-quark decays $t \rightarrow uh, ch$ in $pp \rightarrow t\bar{t}$ events at a center of mass energy of 13 TeV and with 36.1 fb^{-1} [56]. They found $BR(t \rightarrow uh) < 2.4 \cdot 10^{-3}$ and $BR(t \rightarrow ch) < 2.2 \cdot 10^{-3}$.

Using Eq. 40, we have (for $m_{u,c}/m_t \rightarrow 0$):

$$BR(t \rightarrow uh, ch) \approx \frac{m_t \left(1 - \frac{m_b^2}{m_t^2}\right)}{16\pi\Gamma_t} \cdot \xi_{tu,tc}^2 \sim 0.57 \xi_{tu,tc}^2 \quad (43)$$

where Γ_t is the total width of the top-quark.

Thus, the above cited ATLAS bounds translate into the bounds $\xi_{tu}, \xi_{tc} \lesssim 0.06$, allowing FC tuh and tch couplings about 3 times larger than the b-quark Yukawa coupling, i.e., $\xi_{tu}, \xi_{tc} \lesssim 3y_b^{SM}$, which do not rule out the UEHiggsY paradigm with the values $\xi_{tu}, \xi_{tc} \sim y_b^{SM}$.

In Table II we summarize our predictions for the Higgs signals considered in this chapter in the UEHiggsY framework, as well as the corresponding SM predictions and the current limits and sensitivities to some of these signals from the LHC RUN2.

VI. SUMMARY

We have proposed a new framework where the Yukawa couplings of the light quarks of the 1st and 2nd generations, $q = u, d, c, s$, can be as large as the b -quark Yukawa, thus decoupling them from the SM Higgs mechanism, within which a Yukawa coupling of a fermion is proportional to its mass. We have shown that this scenario (which we named the “UEHiggsY paradigm”) is natural, if the typical scale of the NP which is responsible for the enhancement of the light quarks Yukawa couplings is around 1-2 TeV and the heavy (and decoupled) degrees of freedom in the underlying theory have natural couplings of $\mathcal{O}(1)$ with the SM quarks. We have studied the UEHiggsY paradigm in an EFT setup, where dimension six effective operators yield a Yukawa term $y_q \sim \mathcal{O}\left(f \frac{v^2}{\Lambda^2}\right)$, where Λ is the typical NP scale and f is a dimensionless coefficient (i.e., the Wilson coefficient in the EFT expansion), which depends on the properties and details of the underlying NP dynamics. In particular, with $\Lambda \sim \mathcal{O}(1)$ TeV and natural Wilson coefficients $f \sim \mathcal{O}(1)$, one obtains $y_q \sim \mathcal{O}(\text{few } 10^{-2}) \sim \mathcal{O}(y_b^{SM})$.

We also explore the UEHiggsY scenario in extensions of the SM which contain TeV-scale vector-like quarks (VLQ) with a typical mass of 1-2 TeV, which we matched to the higher dimensional EFT operators. We then discuss the flavor structure of the UEHiggsY Yukawa textures and, in particular, of the VLQ extension, and the sensitivity of the measured 125 GeV Higgs signals to this paradigm.

Finally, we suggest some “smoking gun” signals of the UEHiggsY paradigm that should be accessible to the future LHC runs: multi-Higgs production $pp \rightarrow hh, hhh$ and single Higgs production in association with a high p_T jet or photon $pp \rightarrow hj, h\gamma$ and with a single top-quark $pp \rightarrow ht$.

Acknowledgments: We thank Jose Wudka and Arvind Rajaraman for useful discussions. The work of

		$\sqrt{s} = 13$ TeV (RUN2)		
Higgs signal	SM prediction	our UEHiggsY prediction	Current limit/sensitivity	
$R_{hV \rightarrow b\bar{b}V} = \frac{\sigma(pp \rightarrow hV \rightarrow b\bar{b}V)}{\sigma(pp \rightarrow hV \rightarrow b\bar{b}V)_{SM}}$ $V = Z, W$	1	~ 0.33	$\sim 0.9 \pm 0.3$ (ATLAS [33]) $\sim 1.06 \pm 0.3$ (CMS [34])	
$R_{hj \rightarrow f\bar{f}j} = \frac{\sigma(pp \rightarrow hj \rightarrow f\bar{f}+j)}{\sigma(pp \rightarrow hj \rightarrow f\bar{f}+j)_{SM}}$ $f = b, \tau, \gamma, Z, W$ $p_T(h) > 200$ GeV	1	$\sim 0.3 - 0.4$	None	
$\sigma(pp \rightarrow h\gamma)$ $p_T(\gamma) > 30$ GeV	~ 0.1 [fb]	~ 1.25 [pb]	None	
$\sigma(pp \rightarrow ht)$	~ 0	~ 100 [fb]	$\lesssim 1.5$ [pb] (CMS [55])	
$R_{hh} = \frac{\sigma(pp \rightarrow hh)}{\sigma(pp \rightarrow hh)_{SM}}$	1	~ 100	None	
$R_{hh \rightarrow b\bar{b}\gamma\gamma}$	1	~ 10	$\lesssim 19$ (CMS [47])	
$R_{hh \rightarrow b\bar{b}b\bar{b}}$	1	~ 10	$\lesssim 29$ (ATLAS [48])	
$R_{hhh} = \frac{\sigma(pp \rightarrow hhh)}{\sigma(pp \rightarrow hhh)_{SM}}$	1	~ 300	None	
$R_{hhh \rightarrow b\bar{b}b\bar{b}b\bar{b}}$	1	~ 10	None	

TABLE II: Some “smoking gun” Higgs signals of the UEHiggsY paradigm at the LHC with c.m. energy of 13 TeV. Also listed are the corresponding SM predictions and the current limits and sensitivities (from the LHC RUN2) to some of the signals. The cases where we did not find an experimental bound/measurement are marked by “None”. The LHC experimental groups are encouraged to perform a dedicated search in these channels, e.g., the exclusive $pp \rightarrow h\gamma$, which may also be important for the search of heavy resonances [57].

AS was supported in part by the US DOE contract #DE-SC0012704.

[1] A.L. Kagan, G. Perez, F. Petriello, Y. Soreq, S. Stoynev, J. Zupan, Phys.Rev.Lett. **114** (2015), 101802, arXiv:1406.1722 [hep-ph].

[2] G. Perez, Y. Soreq, E. Stamou, K. Tobioka, Phys.Rev. **D92** (2015), 033016, arXiv:1503.00290 [hep-ph].

[3] G. Perez, Y. Soreq, E. Stamou, K. Tobioka1, Phys.Rev. **D93** (2016), 013001, arXiv:1505.06689 [hep-ph].

[4] Y. Soreq, H.X. Zhu, J. Zupan, JHEP **1612** (2016) 045, arXiv:1606.09621 [hep-ph];

[5] F. Yu, JHEP **1702** (2017) 083, arXiv:1609.06592 [hep-ph].

[6] F. Bishara, U. Haisch, P.F. Monni, E. Re, Phys.Rev.Lett. **118** (2017), 121801, arXiv:1606.09253 [hep-ph].

[7] S. Jana, S. Nandi, Phys.Lett. **B783** (2018) 51, arXiv:1710.00619 [hep-ph].

[8] A. Banerjee, G. Bhattacharyya, N. Kumar, T.S. Ray, JHEP **1803** (2018) 062, arXiv:1712.07494 [hep-ph].

[9] See e.g., F.J. Botella, G.C. Branco, Miguel Nebot, M.N. Rebelo and J.I. Silva-Marcos, Eur.Phys.J. **C77** (2017) no.6, 408, arXiv:1610.03018 [hep-ph]; G.C. Branco and M.N. Rebelo, J.Phys.Conf.Ser. **873** (2017) no.1, 012011, arXiv:1704.06993 [hep-ph].

[10] F. del Aguila, M. Perez-Victoria, J. Santiago, JHEP **0009** (2000) 011, hep-ph/0007316.

[11] F. del Aguila, J.A. Aguilar-Saavedra, R. Miquel, Phys. Rev. Lett. **82** (1999) 1628; J.A. Aguilar-Saavedra, Phys. Rev. **D67** (2003) 035003, [Erratum: Phys. Rev. **D69** (2004) 099901].

[12] S. Dawson, E. Furlan, Phys. Rev. **D86** (2012) 015021.

[13] S. Fajfer, A. Greljo, J.F. Kamenik, I. Mustac, JHEP **1307** (2013) 155, arXiv:1304.4219 [hep-ph].

[14] J.A. Aguilar-Saavedra, R. Benbrik, S. Heinemeyer, M. Prez-Victoria, Phys.Rev. **D88** (2013) no.9, 094010, arXiv:1306.0572 [hep-ph].

[15] S.A.R. Ellis, R.M. Godbole, S. Gopalakrishna, J.D. Wells, JHEP **1409** (2014) 130, arXiv:1404.4398 [hep-ph].

[16] C.-Yi Chen, S. Dawson, I.M. Lewis, Phys. Rev. **D90** (2014) no.3, 035016, arXiv:1406.3349 [hep-ph].

[17] C.-Yi Chen, S. Dawson, E. Furlan, Phys.Rev. **D96** (2017) no.1, 015006, arXiv:1703.06134 [hep-ph].

[18] D. Barducci, L. Panizzi, JHEP **1712** (2017) 057, arXiv:1710.02325 [hep-ph].

[19] S. Raby, A. Trautner, arXiv:1712.09360 [hep-ph].

[20] S. Bar-Shalom, A. Soni, J. Wudka, Phys.Rev. **D92** (2015) no.1, 015018, arXiv:1405.2924 [hep-ph]; S. Bar-Shalom, Nucl.Part.Phys.Proc. **273-275** (2016) 696-702, arXiv:1410.3848 [hep-ph].

[21] K.S. Babu, I. Gogoladze, M. Ur Rehman, Q. Shafi, Phys.Rev. **D78** (2008) 055017 arXiv:0807.3055 [hep-ph]; P. W. Graham, A. Ismail, S. Rajendran, P. Saraswat, Phys.Rev. **D81** (2010) 055016, arXiv:0910.3020 [hep-ph].

[22] M. Schmaltz, D. Tucker-Smith, Ann.Rev.Nucl.Part.Sci. **55** (2005) 229, hep-ph/0502182 and references therein.

[23] C. Delaunay, C. Grojean, G. Perez, JHEP **1309** (2013) 090, arXiv:1303.5701 [hep-ph].

[24] C. Delaunay, T. Flacke, J. Gonzalez-Fraile, Seung J. Lee, G. Panico, G. Perez, JHEP **1402** (2014) 055, arXiv:1311.2072 [hep-ph].

[25] F. del Aguila, M.K. Chase, J. Cortes, Nucl. Phys. **B271** (1986) 61; G.C. Branco, L.avoura, Phys.

Lett. **B278** (1986) 738; L. Bento, G.C. Branco, Phys. Lett. **B245** (1990) 599; L. Bento, G.C. Branco, P.A. Parada, Phys. Lett. **B267** (1991) 95; L. Lavoura, J.P. Silva, Phys. Rev. **D47** (1993) 1117; G.C. Branco, P.A. Parada, M.N. Rebelo, hep-ph/0307119; G. Barenboim, F.J. Botella, O. Vives, Nucl. Phys. **B613** (2001) 285, hep-ph/0105306; J.A. Aguilar-Saavedra, F.J. Botella, G.C. Branco, M. Nebot, Nucl. Phys. **B706** (2005) 204, hep-ph/0406151; F.J. Botella, G.C. Branco, M. Nebot, Phys. Rev. **D79** (2009) 096009, arXiv:0805.3995 [hep-ph]; K. Higuchi, K. Yamamoto, Phys. Rev. **D81** (2010) 015009, arXiv:0911.1175 [hep-ph]; F.J. Botella, G.C. Branco, M. Nebot, JHEP **1212** (2012) 040, arXiv:1207.4440 [hep-ph]; A.K. Alok, S. Banerjee, D. Kumar, S.U. Sankar, D. London, Phys. Rev. **D92** (2015) 013002, arXiv:1504.00517 [hep-ph]; K. Ishiwata, Z. Ligeti, M.B. Wise, JHEP **1510** (2015) 027, arXiv:1506.03484 [hep-ph]; C. Bobeth, A.J. Buras, A. Celis, M. Jung, arXiv:1609.04783 [hep-ph]. G. Abbas, arXiv:1712.08052 [hep-ph].

[26] See e.g., “Search for new heavy quarks in ATLAS”, talk given in the 53rd Rencontres de Moriond - EW 2018, by N. Nikiforou (on behalf of the ATLAS collaboration).

[27] G. Blankenburg, J. Ellis, G. Isidori, Phys.Lett. **B712** (2012) 386, arXiv:1202.5704 [hep-ph].

[28] “Measurements of the Higgs boson production and decay rates and constraints on its couplings from a combined ATLAS and CMS analysis of the LHC pp collision data at $\sqrt{s} = 7$ and 8 TeV”, ATLAS and CMS Collaborations, G. Aad *et al.*, JHEP **1608** (2016) 045, arXiv:1606.02266 [hep-ex].

[29] H. Mantler, M. Wiesemann, Eur. Phys. J. **C73** (2013), 2467, arXiv:1210.8263 [hep-ph];

[30] C. Mariotti, G. Passarino, Int.J.Mod.Phys. **A32** (2017) no.04, 1730003, arXiv:1612.00269 [hep-ph].

[31] A. Djouadi, Phys.Rept. **457** (2008) 1, hep-ph/0503172.

[32] See e.g., “Measurements of the Higgs boson”, by P. Meridiani, talk given at the EPS conference on High Energy Physics, Venice, Italy 5-12 July 2017.

[33] M. Aaboud *et al.*, the ATLAS Collaboration, JHEP **1712** (2017) 024, arXiv:1708.03299 [hep-ex].

[34] “Evidence for the decay of the Higgs Boson to Bottom Quarks”, the CMS collaboration, CMS-PAS-HIG-16-044.

[35] See e.g., S. Dawson, A. Ismail, I. Low, Phys. Rev. **D91** (2015) no.11, 115008, arXiv:1504.05596 [hep-ph]; E. Asakawa, D. Harada, S. Kanemura, Y. Okada, K. Tsumura, Phys.Rev. **D82** (2010) 115002, arXiv:1009.4670 [hep-ph]; G. D. Kribs, A. Martin, Phys.Rev. **D86** (2012) 095023, arXiv:1207.4496 [hep-ph].

[36] S. Dawson, S. Dittmaier, M. Spira, Phys.Rev. **D58** (1998) 115012, hep-ph/9805244; D. de Florian, J. Mazzitelli, Phys.Rev.Lett. **111** (2013) 201801, arXiv:1309.6594 [hep-ph]; S. Borowka, N. Greiner, G. Heinrich, S. Jones, M. Kerner, J. Schlenk, U. Schubert, T. Zirke, Phys.Rev.Lett. **117** (2016) 012001, [Erratum-ibid. **117** (2016) 079901], arXiv:1604.06447 [hep-ph]; S. Borowka, N. Greiner, G. Heinrich, S.P. Jones, M. Kerner, J. Schlenk, T. Zirke, JHEP **1610** (2016) 107, arXiv:1608.04798 [hep-ph]; S. Borowka (Zurich U.), G. Heinrich, S. Jahn, S.P. Jones, M. Kerner, J. Schlenk, T. Zirke, J.Phys.Conf.Ser. **762** (2016) no.1, 012073, arXiv:1604.00267 [hep-ph]; D. de Florian and J. Mazzitelli, JHEP **09** (2015) 053, arXiv:1505.07122 [hep-ph]; G. Degrassi, P. P. Giardino, and R. Grber, Eur.Phys.J. **C76** (2016) 411, arXiv:1603.00385 [hep-ph]; J. Grigo, J. Hoff, and M. Steinhauser, Nucl.Phys. **B900** (2015) 412, arXiv:1508.00909 [hep-ph].

[37] See e.g., C. Anastasiou *et al.*, JHEP **05**, 058 (2016), arXiv:1602.00695 [hep-ph].

[38] See e.g., R. V. Harlander, Eur.Phys.J. **C76** (2016) no.5, 252, arXiv:1512.04901 [hep-ph].

[39] J. Alwall, R. Frederix, S. Frixione, V. Hirschi, F. Maltoni, O. Mattelaer, H.S. Shao, T. Stelzer, P. Torrielli, M. Zaro, JHEP **07** (2014), 079, arXiv:1405.0301 [hep-ph].

[40] A. Alloul *et al.*, Comput.Phys.Commun. **185** (2014), 2250, arXiv:1310.1921 [hep-ph].

[41] J. Cohen, S. Bar-Shalom, G. Eilam and A. Soni, Phys. Rev. **D97** (2018) no.5, 055014, arXiv:1705.09295 [hep-ph].

[42] See e.g., Handbook of LHC Higgs Cross Sections: 4. Deciphering the Nature of the Higgs Sector LHC Higgs Cross Section Working Group, D. de Florian *et al.*, arXiv:1610.07922 [hep-ph].

[43] C. Grojean, E. Salvioni, M. Schlaffer, A. Weiler, JHEP **1405** (2014) 022, arXiv:1312.3317 [hep-ph].

[44] M. Buschmann, C. Englert, D. Goncalves, T. Plehn, M. Spannowsky, Phys.Rev. **D90** (2014) no.1, 013010, arXiv:1405.7651 [hep-ph].

[45] N. Deutschmann, C. Duhr, F. Maltoni, E. Vryonidou, JHEP **1712** (2017) 063, Erratum: JHEP **1802** (2018) 159, arXiv:1708.00460 [hep-ph].

[46] S. Jana, S. Nandi, arXiv:1710.00619 [hep-ph].

[47] See talk at the EPS-HEP 2017, “Searches for HH production at 13 TeV with the CMS detector”, by Martino DallOsso (on behalf of CMS collaboration).

[48] See talk at the EPS-HEP 2017 “Search for di-Higgs production with the ATLAS detector”, by Will Davey (on behalf of the ATLAS Collaboration).

[49] A. Abbasabadi, D. Bowser-Chao, D.A. Dicus, W.W. Repko, Phys.Rev. **D58** (1998) 057301, hep-ph/9706335.

[50] E. Gabrielli, B. Mele, F. Piccinini, R. Pittau, JHEP **1607** (2016) 003, arXiv:1601.03635 [hep-ph].

[51] E. Gabrielli, F. Maltoni, B. Mele, M. Moretti, F. Piccinini, R. Pittau, Nucl. Phys. **B781** (2007) 64, hep-ph/0702119.

[52] H. Khanpour, S. Khatibi, M.M. Najafabadi, Phys.Lett. **B773** (2017) 462, arXiv:1702.05753 [hep-ph].

[53] S. Biswas, E. Gabrielli, B. Mele, JHEP **1301** (2013) 088, arXiv:1211.0499 [hep-ph].

[54] See e.g., G. Eilam, J.L. Hewett, A. Soni, Phys.Rev. **D44** (1991) 1473, Erratum: Phys.Rev. **D59** (1999) 039901.

[55] A.M. Sirunyan *et al.*, the CMS Collaboration, “Search for the flavor-changing neutral current interactions of the top quark and the Higgs boson which decays into a pair of b quarks at $\sqrt{s} = 13$ TeV”, arXiv:1712.02399 [hep-ex].

[56] The ATLAS Collaboration, “Search for top quark decays $t \rightarrow qH$, with $H \rightarrow \gamma\gamma$, in $\sqrt{s} = 13$ TeV pp collisions using the ATLAS detector”, JHEP **1710** (2017) 129, arXiv:1707.01404 [hep-ex].

[57] See e.g., N. Craig, P. Draper, K. Kong, Y. Ng, D. Whiteson, arXiv:1610.09392 [hep-ph]; B.A. Dobrescu, P.J. Fox, J. Kearney, Eur.Phys.J. **C77** (2017) no.10, 704, arXiv:1705.08433 [hep-ph].